RESEARCH ARTICLE

Semi-synthetic cinnamodial analogues: Structural insights into the insecticidal and antifeedant activities of drimane sesquiterpenes against the mosquito *Aedes aegypti*

Preston K. Manwill[1,2], **Megha Kalsi**[3], **Sijin Wu**[1], **Erick J. Martinez Rodriguez**[3], **Xiaolin Cheng**[1]*, **Peter M. Piermarini**[2,3]*, **Harinantenaina L. Rakotondraibe**[1,2]*

1 Division of Medicinal Chemistry and Pharmacognosy, College of Pharmacy, The Ohio State University, Columbus, Ohio, United States of America, **2** Center for Applied Plant Sciences, The Ohio State University, Columbus, Ohio, United States of America, **3** Department of Entomology, The Ohio State University, Ohio Agricultural Research and Development Center, Wooster, Ohio, United States of America

* cheng.1302@osu.edu (XC); piermarini.1@osu.edu (PMP); rakotondraibe.1@osu.edu (HLR)

Abstract

The *Aedes aegypti* mosquito serves as a major vector for viral diseases, such as dengue, chikungunya, and Zika, which are spreading across the globe and threatening public health. In addition to increased vector transmission, the prevalence of insecticide-resistant mosquitoes is also on the rise, thus solidifying the need for new, safe and effective insecticides to control mosquito populations. We recently discovered that cinnamodial, a unique drimane sesquiterpene dialdehyde of the Malagasy medicinal plant *Cinnamosma fragrans*, exhibited significant larval and adult toxicity to *Ae. aegypti* and was more efficacious than DEET–the gold standard for insect repellents–at repelling adult female *Ae. aegypti* from blood feeding. In this study several semi-synthetic analogues of cinnamodial were prepared to probe the structure-activity relationship (SAR) for larvicidal, adulticidal and antifeedant activity against *Ae. aegypti*. Initial efforts were focused on modification of the dialdehyde functionality to produce more stable active analogues and to understand the importance of the 1,4-dialdehyde and the α,ß-unsaturated carbonyl in the observed bioactivity of cinnamodial against mosquitoes. This study represents the first investigation into the SAR of cinnamodial as an insecticide and antifeedant against the medically important *Ae. aegypti* mosquito.

Author summary

Aedes mosquitoes are the primary carriers of Zika, dengue, chikungunya, and yellow fever viruses around the globe. Given the emergence of insecticide-resistance in this genus and unprecedented 'globalization' of mosquito-borne viruses, new chemicals to control these mosquitoes (e.g., insecticides, repellents) are urgently needed. In the continuation of our search for new and safe natural product derived insecticides, we generated semi-synthetic

derivatives of cinnamodial (CDIAL), previously identified as an insect antifeedant, repellent and insecticide, to give insights into the important features of the molecule that can contribute to the observed activities. Since the antifeedant and repellent activity of CDIAL are found to be mediated by modulation of a sensory receptor (TRPA1) in the mosquito, we developed a structural model to understand how CDIAL interacts with TRPA1 and to explain the difference in activities of CDIAL and the prepared derivatives. Our findings aid in the development of plant-derived insecticides to control the *Ae. aegypti* mosquito and justify continued efforts using TRPA1 as a target for new mosquito repellents.

Introduction

Mosquitoes are vectors of numerous human pathogens, such as the malaria parasite, dengue virus, chikungunya virus, and Zika virus, which affect over 300 million people annually [1–3]. While the majority of the burden has been shouldered by Africa and South-East Asia the global disease distribution is widening. The worldwide incidence of dengue has risen 30-fold in the past 30 years, and more countries are reporting their first outbreak of the disease [3]. Chikungunya and Zika viruses, both historically limited to parts of Africa and Asia, have recently emerged into global threats with increased transmission in the Americas [4,5]. The arboviruses that cause dengue, Zika, chikungunya and yellow fevers can all be transmitted to humans by the mosquito *Aedes aegypti* (L.). According to the World Health Organization more than half of the world's population lives in areas where this mosquito species is present, including several southern regions in the United States [2]. While significant progress has been made in developing therapeutics and vaccines for mosquito-borne pathogens, more effective and low-cost means to treat and prevent these diseases are still underdeveloped or unavailable [6,7]. Vector control strategies remain the primary method to control and prevent the spread of mosquito-borne diseases [8]; chiefly, control of mosquitoes with insecticides is often the only method proven to reduce vector populations during an emerging epidemic [9].

The major classes of insecticides used in vector control strategies include the pyrethroids, carbamates, organophosphates, and neonicotinoids, which all target the nervous system of insects [10–13]. While their activity has made them very effective at reducing mosquito populations, they are non-selective, killing beneficial insects and in some cases small vertebrate animals, which has caused the removal of some agents such as DDT and other organochlorine compounds from the vector control arsenal [14]. Excessive use of the remaining groups of insecticides, however, has led to the selection of insecticide-resistant mosquito populations [15–17]. Moreover, no new public health insecticides have been developed in the past 40 years [18]. Thus, it is imperative that we replenish our chemical toolbox by identifying new agents that exhibit novel mechanisms of action with high selectivity to mosquitoes.

Plants have been an indispensable source of novel compounds possessing pharmacological activities relevant to public health [10]. Pyrethroids, for instance, the most widely used insecticides in the United States and the only class approved for insecticide treated nets [19], are derived from natural pyrethrins isolated from the flowers of *Tanacetum cinerariifolium* (Trevir.) Sch.Bip. (Asteraceae) [20]. Recently, we have identified that an extract of *Cinnamosma fragrans* Baill. (Canellaceae), a plant used in Malagasy traditional medicine, is antifeedant, repellent, and toxic to *Ae. aegypti* mosquitoes. In our efforts to isolate and characterize the bioactive compounds from *C. fragrans*, we identified cinnamodial (CDIAL, **1**), a drimane sesquiterpene with promising toxicity to larval and adult female *Ae. aegypti* mosquitoes [21]. In addition to exhibiting a similar toxic profile against pyrethroid-susceptible and -resistant

strains of *Ae. aegypti*, CDIAL was more efficacious than DEET [N,N-Diethyl-meta-toluamide]–the gold standard for insect repellents–at repelling mosquitoes from feeding on blood [21]. Moreover, we demonstrated that the mechanism of the antifeedant activity of CDIAL was through the activation of transient receptor potential A1 (TRPA1) channels [21].

The goal of the present study was to investigate the structural basis of the insecticidal and antifeedant activities of **1** against *Ae. aegypti* by generating a series of semi-synthetic CDIAL derivatives. Our efforts led to the discovery of **10** ((-)-6ß-Acetoxy-9α-hydroxydrim-7-ene-12-methyl-12-one-11-al) as a CDIAL derivative with superior and similar insecticidal activity against larvae and adult females, respectively, but weaker antifeedant activity against adult females. Herein, we describe the re-isolation of **1**, analog generation, and biological evaluation of synthetic derivatives. Additionally, in order to understand the mechanisms of the most active compounds, the observed structure-activity relationship (SAR) and potential interaction of the active compounds with several nucleophilic residues of the mosquito TRPA1 are discussed.

Methods

General experimental procedures

Optical rotations ($[\alpha]_D$) were measured with an LED light source monitoring at 589 nm in acetonitrile at 20 °C. The instrument used was an Anton Paar MCP 150 polarimeter (Anton Paar OptoTec GmbH, Seelze-Letter, Germany). Ultraviolet (UV) absorption spectra were measured in a 1 cm quartz tank using a Hitachi U-2910 UV/vis double-beam spectrophotometer (Hitachi High-Technologies America, Schaumburg, IL, USA). Infrared (IR) spectra were obtained on a Nicolet 6700 FT-IR spectrometer (Thermo Scientific, Waltham, MA, USA). The 1D (^{1}H, ^{13}C, selective COSY and NOESY) and 2D (COSY, HSQC, HMBC, and NOESY) NMR spectra were recorded at 300 K (26.85 °C) in CDCl$_3$ for all compounds except for **5** and **19** which were measured in methanol-d_4, **7** which was measured in acetonitrile-d_3, and **16** was measured in pyridine-d_5 on a Bruker Avance III HD 400 MHz instrument (Bruker, Billerica, MA, USA) using standard Bruker pulse sequences. ^{1}H chemical shifts are reported in parts per million (ppm) and are referenced to the residual CDCl$_3$ signal (δ 7.26 ppm), methanol-d_4 signal (δ 3.34 ppm), pyridine-d_5 signal (δ 7.22 ppm), or acetonitrile-d_3 signal (δ 1.96 ppm). ^{13}C chemical shifts are reported in ppm and are referenced to the residual CDCl$_3$ signal (δ 77.36 ppm), methanol-d_4 signal (δ 49.86 ppm), pyridine-d_5 signal (δ 123.87 ppm) or acetonitrile-d_3 signal (δ 118.77 ppm). Deuterated NMR solvents were purchased from Cambridge Isotope Laboratories (Tewksbury, MA, USA). High-resolution mass spectra (HRESIMS) were acquired on a hybrid spectrometer utilizing a linear ion trap and Orbitrap (LTQ Orbitrap, ThermoFisher Scientific Inc., Bremen, Germany) equipped with an ESI source in the positive-ion mode, with sodium iodide (NaI) being used for mass calibration. The spectrometer was equipped with an Agilent 1100 HPLC system (Agilent Technologies, California, USA) including a binary pump, UV detector, and autosampler. Data acquisition and analysis were accomplished with Xcalibur software version 2.0 (Thermo Fisher Scientific Inc., Bremen, Germany). The samples were prepared at a concentration of ~10 μg/mL in ACN, and the injection volume was set at 30 μL. Flash and open-column chromatography were performed with SilicaFlash P60 (230–400 mesh; SiliCycle Inc., Quebec City, Canada) using solvent systems as described. Ratios of solvent systems used for chromatography are expressed in v/v as specified. Analytical thin-layer chromatography was performed on aluminum-backed precoated silica gel plates (0.24 mm; Dynamax Adsorbant, Inc., Darmstadt, Germany). Spots were visualized under UV light (254 & 320) and by spraying with modified Godin's reagent (vanillin/EtOH-Perchloric acid, 1:1, v/v) and H$_2$SO$_4$-water (15%) followed by heating. Commercially available chemicals were used

as purchased. Ice/water was used as the temperature bath to achieve 0˚C and dry ice/acetone was used to achieve −78 ^{o}C. Dry tetrahydrofuran (THF) and dichloromethane (CH_2Cl_2) were obtained from an Innovative Technology PureSolv system (Inert, Massachusetts, USA). Unless otherwise noted, reactions were performed in oven-dried glassware under an atmosphere of dry argon.

Plant material

The stem bark of *C. fragrans* was purchased at the market of traditional medicines, Analakely/ Antananarivo, (Madagascar). The bark was identified by comparison with the authentic sample in the Herbarium of PBZT (Parc Botaniqueet Zoologique de Tsimbazaza, Antananarivo, Madagascar). A voucher specimen of the bark (LivCF2016) was deposited at the College of Pharmacy, The Ohio State University (Columbus, Ohio).

Extraction and isolation

The air-dried stem bark of *C. fragrans* was pulverized and the powder (400 g) was extracted with dichloromethane for 5 days at room temperature. The extract was filtered and concentrated *in vacuo* to yield a yellow-brown oily residue (80.68 g, 20.2% on dry plant material). The residue was divided into fractions using column chromatography over silica gel, eluting with a gradient system of hexanes–EtOAc (from 4:1 to 0:1). Cinnamodial (**1**) was recrystallized using hexanes–EtOAc (1:1) as colorless crystals (5.28 g, 1.32% on dry plant material).

Synthesis

The following cinnamodial analogues were prepared according to the semi-synthetic methods described in the supporting information: cinnamodiacid (**5**), cinnamodimethylester (**6**), cinnamo-N,11-dihydro-11-pyridazinol (**7**), 7*ß*-hydroxy-cinnamopyridazine (**18**), and Cinnamodial 12-ethylene acetal (**11**). The preparation of 6-*O*-acetyl-12*α*-methyl-pereniporin A (**8**), 6-*O*-acetyl-12*ß*-methyl-pereniporin A (**9**), (−)-6*ß*-Acetoxy-9*α*-hydroxydrim-7-ene-12-methyl-12-one-11-al (**10**), 12*α*/*ß*-methyl-pereniporin A (**12**), (1'*S/R*)-1'-((8a*S*)-5,5,8a-trimethyl-1,4-dioxo-1,4,4a,5,6,7,8,8a-octahydronaphthalene-2-yl)ethyl formate (**13**), and Cinnamothiazolidine (**16**) are described below.

6-*O*-acetyl-12*α*-methyl-pereniporin A (8) and 6-*O*-acetyl-12*ß*-methyl-pereniporin A (9). To a solution of **1** (50 mg, 0.16 mmol) in dry THF (1 mL), methylmagnesium bromide (36.4 mg, 0.486 mmol, 3 equiv) in THF (162 μL) was added dropwise at −78 ^{o}C. The reaction mixture was maintained at this temperature, with stirring for 30 min, after which it was allowed to reach r.t. and maintained for another 1.5 h. The reaction mixture was then quenched with NH_4Cl (1 mL of a saturated aqueous solution). The aqueous solution was extracted with EtOAc (2 mL × 3) and the combined organic layers dried over anhydrous $MgSO_4$, filtered, and concentrated. The resulting residue was purified by column chromatography with hexanes–EtOAC (from 3:1 to 2:1) as eluents to afford two diastereomeric compounds **8** and **9**.

Compound **8** (7.14 mg, 14%) as a colorless oil: $[\alpha]_D^{20}$ −165 (*c* 1, ACN); IR (KBr) ν_{max} 3427, 2948, 2931, 2869, 1735, 1463, 1372, 1242, 1069, 1024, 983, 960, and 756 cm^{-1}; ^{1}H NMR (400 MHz, $CDCl_3$) δ 5.65 (1H, dd, *J* = 4.0, 1.7 Hz, H-7), 5.61 (1H, td, *J* = 4.4, 1.4 Hz, H-6), 5.27 (1H, s, H-11), 4.41 (1H, qt, *J* = 6.6, 1.6 Hz, H-12), 3.90 (1H, d, *J* = 10.4, 11-OH), 2.05 (3H, s, H-17), 2.03 (1H, d, *J* = 4.0 Hz, H-5), 1.88 (1H, td, *J* = 13.3, 4.4 Hz, H-1*α*), 1.63 (1H, qt, *J* = 13.5, 3.2 Hz, H-2*ß*), 1.50 (1H, dquint *J* = 13.8, 3.4 Hz, H-2*α*), 1.40 (1H, overlapped, H-1*ß*), 1.39 (3H, d, *J* = 6.6 Hz, 12-CH$_3$), 1.38 (1H, overlapped, H-3*ß*), 1.27 (1H, td, *J* = 13.0, 2.9 Hz, H-3*α*), 1.16

(3H, s, H-15), 1.15 (3H, s, H-14), 0.99 (3H, s, H-13); ^{13}C NMR (100 MHz, CDCl$_3$) δ 170.7 (C = O, C-16), 146.6 (C, C-8), 120.9 (CH, C-7), 98.1 (CH, C-11), 78.5 (C, C-9), 73.3 (CH, C-12), 67.7 (CH, C-6), 45.9 (CH, C-5), 45.0 (CH$_2$, C-3), 38.8 (C, C-10), 34.0 (C, C-4), 33.3 (CH$_3$, C-13), 31.9 (CH$_2$, C-1), 24.9 (CH$_3$, C-14), 23.0 (CH$_3$ at C-12), 22.0 (CH$_3$, C-17), 19.1 (CH$_3$, C-15), 18.3 (C, C-2); HRESIMS *m/z* 347.18280 [M + Na]$^+$ (calcd for C$_{18}$H$_{28}$O$_5$Na, 347.18290).

Compound **9** (21.26 mg, 40%) as a yellow oil: $[\alpha]_D^{20}$ −90 (*c* 1, CH$_3$CN); IR (KBr) ν_{max} 3434, 2949, 2925, 2868, 1737, 1721, 1462, 1445, 1371, 1242, 1218, 1068, 1022, 986, 958, 913, and 756 cm^{-1}; ^{1}H NMR (400 MHz, CDCl$_3$) δ 5.62 (1H, td, *J* = 4.4, 2.0 Hz, H-6), 5.51 (1H, dd, *J* = 4.0, 2.1 Hz, H-7), 5.39 (1H, s, H-11), 4.77 (1H, qt, *J* = 6.2, 2.1 Hz, H-12), 2.06 (3H, s, H-17), 2.04 (1H, d, *J* = 4.0 Hz, H-5), 1.85 (1H, td, *J* = 13.2, 4.4 Hz, H-1α), 1.64 (1H, qt, *J* = 13.4, 3.1 Hz, H-2ß), 1.50 (1H, dquint *J* = 13.8, 3.4 Hz, H-2α), 1.37 (1H, overlapped, H-3ß), 1.28 (1H, overlapped, H-1ß), 1.27 (1H, overlapped, H-3α), 1.26 (3H, d, *J* = 6.1 Hz, 12-CH$_3$), 1.14 (3H, s, H-14), 1.11 (3H, s, H-15), 0.98 (3H, s, H-13); ^{13}C NMR (100 MHz, CDCl$_3$) δ 170.9 (C = O, C-16), 146.6 (C, C-8), 118.8 (CH, C-7), 96.2 (CH, C-11), 79.3 (C, C-9), 73.3 (CH, C-12), 67.6 (CH, C-6), 45.5 (CH, C-5), 45.0 (CH$_2$, C-3), 38.4 (C, C-10), 33.9 (C, C-4), 33.0 (CH$_3$, C-13), 32.0 (CH$_2$, C-1), 24.8 (CH$_3$, C-14), 22.1 (CH$_3$, C-17), 18.7 (CH$_3$ at C-12), 18.6 (CH$_3$, C-15), 18.3 (C, C-2); HRESIMS *m/z* 347.18276 [M + Na]$^+$ (calcd for C$_{18}$H$_{28}$O$_5$Na, 347.18290).

(−)-6ß-Acetoxy-9α-hydroxydrim-7-ene-12-methyl-12-one-11-al (10). Compound **9** (*ca.* 20 mg, 0.062 mmol) was dissolved in chloroform and left at room temperature for 22 days, concentrated and purified via column chromatography (hexanes–EtOAc 2:1) to yield **10** (4.49 mg, 22%) as a colorless oil: $[\alpha]_D^{20}$ −211 (*c* 1, ACN); UV (ACN) λ_{max} (log ε 3.37) 218 nm; IR (KBr) ν_{max} 3450, 2948, 2930, 2870, 1737, 1673, 1463, 1372, 1233, 1030, 1055, 1030, and 756 cm^{-1}; ^{1}H NMR (400 MHz, CDCl$_3$) δ 9.69 (1H, d, *J* = 0.92 Hz, H-11), 7.00 (1H, d, *J* = 4.9 Hz, H-7), 5.84 (1H, t, *J* = 4.8 Hz, H-6), 4.09 (1H, d, *J* = 1.1, 9-OH), 2.36 (3H, s, 12-CH$_3$), 2.14 (3H, s, H-17), 1.99 (1H, d, *J* = 4.5 Hz, H-5), 1.79 (1H, td, *J* = 13.2, 4.5 Hz, H-1α), 1.61 (1H, overlapped, H-2ß), 1.52 (1H, overlapped, H-2α), 1.38 (1H, overlapped, H-3ß), 1.30 (3H, s, H-15), 1.27 (1H, overlapped, H-3α), 1.15 (3H, s, H-14), 1.05 (1H, overlapped, H-1ß), 1.01 (3H, s, H-13); ^{13}C NMR (100 MHz, CDCl$_3$) δ 200.6 (CH, C-11), 199.8 (C, C-12), 170.6 (C = O, C-16), 141.1 (C, C-8), 140.3 (CH, C-7), 78.3 (C, C-9), 66.7 (CH, C-6), 44.6 (CH, C-5), 44.4 (CH$_2$, C-3), 41.7 (C, C-10), 34.2 (C, C-4), 33.0 (CH$_3$, C-13), 32.3 (CH$_2$, C-1), 25.9 (CH$_3$ at C-12), 25.1 (CH$_3$, C-14), 21.9 (CH$_3$, C-17), 20.2 (CH$_3$, C-15), 18.1 (C, C-2); HRESIMS *m/z* 345.16742 [M + Na]$^+$ (calcd for C$_{18}$H$_{26}$O$_5$Na, 345.16725).

12α/ß-methyl-pereniporin A (12). To a solution of **1** (100 mg, 0.324 mmol) in dry THF (1 mL), methylmagnesium bromide (121.27 mg, 1.621 mmol, 5 equiv) in THF (0.540 mL) was added dropwise at −78 °C. The reaction mixture was maintained at this temperature, with stirring, for 2 h. At this time, it was quenched with NH$_4$Cl (2 mL of a saturated aqueous solution). The aqueous solution was extracted with EtOAc (4 mL × 3) and the combined organic layers washed with brine (4 mL), dried over anhydrous MgSO$_4$, filtered, and concentrated to yield crude **12** (120.68 mg) as a 1:2 diasteromeric mixture of 12α-methyl-pereniporin A and 12ß-methyl-pereniporin A, respectively. IR (KBr) ν_{max} 3415, 2972, 2947, 2924, 2869, 1710, 1461, 1383, 1216, 1081, 1065, 1026, 985, 961, and 757 cm^{-1}; ^{1}H NMR (400 MHz, CDCl$_3$) δ (major isomer, C-12ß) 5.62 (1H, dd, *J* = 4.0, 2.1 Hz, H-7), 5.38 (1H, s, H-11), 4.79 (1H, qt, *J* = 6.3, 2.3 Hz, H-12), 4.55 (1H, td, *J* = 4.5, 2.3 Hz, H-6), 1.85 (1H, td, *J* = 13.3, 4.5 Hz, H-1α), 1.82 (1H, d, *J* = 5.3 Hz, H-5), 1.66 (1H, qt, *J* = 13.5, 3.3 Hz, H-2ß), 1.51 (1H, dquint *J* = 13.3, 3.9 Hz, H-2α), 1.38 (1H, overlapped, H-3ß), 1.34 (3H, s, H-14), 1.32 (3H, d, *J* = 6.2 Hz, 12-CH$_3$), 1.28 (1H, overlapped, H-3α), 1.27 (1H, overlapped, H-1ß), 1.15 (3H, s, H-15), 1.11 (3H, s, H-13); ^{13}C NMR (100 MHz, CDCl$_3$) δ 144.7 (C, C-8), 123.2 (CH, C-7), 96.4 (CH, C-11), 79.7 (C, C-9), 73.2 (CH, C-12), 66.2 (CH, C-6), 46.7 (CH, C-5), 44.9 (CH$_2$, C-3), 38.3 (C, C-10), 34.4 (C, C-

4), 33.2 (CH$_3$, C-13), 32.5 (CH$_2$, C-1), 25.2 (CH$_3$, C-14), 19.3 (CH$_3$, C-15), 18.9 (CH$_3$ at C-12), 18.4 (C, C-2); HRESIMS *m/z* 305.17252 [M + Na]$^+$ (calcd for C$_{16}$H$_{26}$O$_4$Na, 305.17233).

(1'*S*/*R*)-1'-((8a*S*)-5,5,8a-trimethyl-1,4-dioxo-1,4,4a,5,6,7,8,8a-octahydronaphthalene-2-yl)ethyl formate (13). To a stirred solution of **12** (100.2 mg, 0.294 mmol, crude, obtained from Grignard addition) in CH$_2$Cl$_2$ (2 mL) at 0 ^{o}C was added PCC (253 mg, 1.175 mmol). The resulting mixture was warmed to room temperature and stirred for 2 h before it was diluted with EtOAc (4 mL) and filtered through a short pad of Celite. The crude mixture was chromatographed on a silica gel column eluting with hexanes–EtOAc (4:1) to obtain **13** (26.77 mg, 27%) as a mixture of diastereomers (*ca.* 1:2 ratio of C-1'α and C-1'β, respectively). UV (ACN) λ_{max} (log ε 3.74) 240.5 nm; IR (KBr) ν_{max} 2934, 2872, 1729, 1685, 1464, 1380, 1292, 1231, 1166, and 1019 cm^{-1}; ^{1}H NMR (400 MHz, CDCl$_3$) δ (major isomer, C-1'β): 8.02 (1H, d, *J* = 0.49, –-OC<u>H</u>O), 6.54 (1H, d, *J* = 1.1 Hz, H-3), 5.72 (1H, qt, *J* = 6.5, 0.92 Hz, H-1'), 2.57 (1H, s, H-4a), 1.85 (1H, dm, *J* = 9.6 Hz, H-8β), 1.62 (1H, m, overlapped, H-8α), 1.62 (2H, m, H-7β/α), 1.48 (3H, d, *J* = 6.6 Hz, 1'-CH$_3$), 1.43 (1H, dm, *J* = 13.4 Hz, H-6β), 1.24 (3H, s, 5-βCH$_3$), 1.23 (3H, s, 8a-CH$_3$), 1.15 (1H, td, J = 11.2, 4.8 Hz, H-6α), 1.14 (3H, s, 5-αCH$_3$); ^{13}C NMR (100 MHz, CDCl$_3$) δ 203.0 (C, C-4), 199.3 (C, C-1), 160.0 (CH, –OCHO), 148.2 (C, C-2), 135.9 (CH, C-3), 66.4 (CH, C-1'), 61.8 (CH, C-4a), 51.3 (C, C-8a), 42.7 (CH$_2$, C-6), 33.6 (C, C-5), 33.5 (CH$_2$, C-8), 32.7 (CH$_3$, 5-αCH$_3$), 21.9 (CH$_3$, 5-βCH$_3$), 21.8 (CH$_3$, 8a-CH$_3$), 20.5 (CH$_3$ at C-1'), 17.8 (C, C-7); HRESIMS *m/z* 301.14144 [M + Na]$^+$ (calcd for C$_{17}$H$_{24}$O$_7$Na, 301.14103).

Cinnamothiazolidine (16). Cinnamodial (**1**, 25.5 mg, 0.083 mmol) and *L*-cysteine methyl ester HCL (14.2 mg, 0.83 mmol) were added to an NMR tube, followed by addition of pyridine-*d*$_5$ (0.6 mL), vortexed and incubated at 60 ^{o}C for 45 min. The mixture was intermittently monitored throughout the incubation by NMR at 300.0 K. Compound **16** (98% as observed by ^{1}H NMR) was produced after 45 min of incubation. [α]$_D^{20}$ −164 (*c* 1, CH$_3$CN); UV (ACN) λ_{max} (log ε 3.72) 250 nm; IR (KBr) ν_{max} 3367, 2950, 2928, 2867, 1736, 1677, 1460, 1439, 1371, 1239, 1205, 1167, 1031, and 754 cm^{-1}; ^{1}H NMR (400 MHz, C$_5$D$_5$N) δ 5.93 (1H, dd, *J* = 3.9, 1.2 Hz, H-7), 5.90 (1H, br t, *J* = 4.3 Hz, H-6), 5.79 (1H, s, H-12), 5.05 (1H, dd, *J* = 7.2, 1.7 Hz, H-18), 4.77 (1H, s, H-11), 3.54 (1H, s, 19-OCH$_3$), 3.50 (1H, dd, *J* = 10.8, 7.1 Hz, H-20a), 3.40 (1H, dd, *J* = 10.8, 2.0 Hz, H-20b), 2.63 (1H, d, *J* = 4.9 Hz, H-5), 2.44 (1H, td, *J* = 13.6, 4.4 Hz, H-1α), 1.95 (3H, s, H-17), 1.80 (1H, dm, *J* = 13.6 Hz, H-1β), 1.67 (1H, m, H-2β), 1.48 (1H, dquint, *J* = 13.7, 3.5 Hz, H-2α), 1.42 (3H, s, H-15), 1.31 (2H, dm, *J* = 9.2, 2.8 Hz, H-3α/β), 1.20 (3H, s, H-14), 0.97 (3H, s, H-13); ^{13}C NMR (100 MHz, C$_5$D$_5$N) δ 172.5 (C, C-19), 170.6 (C, C-16), 144.9 (C, C-8), 122.9 (CH, C-7), 87.6 (CH, C-11), 78.4 (C, C-9), 72.3 (CH, C-12), 68.2 (CH, C-6), 68.1 (CH, C-18), 52.3 (CH$_3$, 19-OCH$_3$), 45.8 (CH, C-5), 45.4 (CH$_2$, C-3), 39.5 (C, C-10), 35.2 (CH$_2$, C-20), 34.1 (C, C-4), 33.3 (CH$_3$, C-13), 33.0 (CH$_2$, C-1), 25.0 (CH$_3$, C-14), 21.8 (CH$_3$, C-17), 19.7 (CH$_3$, C-15), 19.0 (CH$_2$, C-2); HRESIMS *m/z* 426.19495 [M + H]$^+$ (calcd for C$_{21}$H$_{32}$NO$_6$S, 426.19448), 448.17728 [M + Na]$^+$ (calcd for C$_{21}$H$_{31}$NO$_6$SNa, 426.17643), and base peak is 408.18484 [M− 18 + H]$^+$ (calcd for C$_{21}$H$_{30}$NO$_5$S).

Mosquito cultures and rearing conditions

Eggs of the Liverpool (LVP) strain of *Ae. aegypti* were obtained through the MR4 as part of the BEI Resources Repository, NIAID, NIH (LVP-IB12, MRA-735, deposited by M.Q. Benedict). The eggs of the *Ae. aegypti* were reared to adults as described previously [22].

Toxicology assays

Larval and adult female toxicities were determined by established protocols [21,23,24]. In brief, for larvae, 10 μL of a derivative (10 mM dissolved in 100% acetone) was added to six wells of a 24-well tissue culture plate containing 1 mL of dH$_2$O and five larvae per well,

resulting in a final concentration of 100 μM (1% acetone). The screening concentration (100 μM) was chosen based on preliminary scouting experiments with CDIAL (**1**) that resulted in ~50% efficacy. After 24 h in normal rearing conditions (28°C, 80% relative humidity), the efficacy was assessed by counting the number of larvae per well that did not move after gentle prodding with a micropipette tip or fine insect pin. As a negative and positive control, respectively, the effects of 1% acetone and 100 μM CDIAL were tested in parallel.

For adults, 500 nL of a derivative (3 mM dissolved in 100% acetone) was applied to the thorax of 10 adult females (3–7 days post emergence) to deliver a dose of 1.5 nmol per mosquito. The screening dose (1.5 nmol/mosquito) was chosen based on preliminary scouting experiments with CDIAL (**1**) that resulted in ~50% efficacy. After dosing, the mosquitoes were held under normal rearing conditions in small plastic cages (32 oz. containers) and provided with access to 10% sucrose. After 24 h, the efficacy was assessed by counting the number of treated mosquitoes that were dead or unable to fly. As a negative and positive control, respectively, the effects of 100% acetone and 1.5 nmol CDIAL were tested in parallel.

The toxicity of compound **13** was also tested by direct injection into the hemolymph of adult females using an approach similar to Raphemot *et al*. 2013 [25]. In brief, 500 nL of **13** (3 mM dissolved in phosphate buffered saline, PBS, with 3% DMSO) was injected into the hemolymph with a pulled-glass capillary attached to a Nanoject II injector (Drummond Scientific Company, Broomall, PA) to deliver a dose of 1.5 nmol per mosquito. The efficacy was assessed at 24 h as described above for adult females. As a negative and positive control, respectively, 3% DMSO (in PBS) and 1.5 nmol CDIAL (in PBS with 3% DMSO) were tested in parallel.

For all toxicity experiments, the mean efficacies of the derivatives and CDIAL were adjusted for effects of the negative control using Abbott's correction [26] and compared statistically using a one-way ANOVA (Bonferroni post-test) or unpaired t-test ($P < 0.05$).

Antifeedant assays

A capillary feeding (CAFE) choice assay was used to determine the antifeedant activity of the compounds [21,27,28]. In brief, groups of 5 adult female mosquitoes (3–10 days post-emergence) were placed in *Drosophila* vials (28.5 x 95 mm) covered with cotton plugs. Two 5-μL calibrated glass capillaries were inserted through the cotton into the vial. One capillary was designated the 'control' and filled with 5 μL of 10% sucrose containing 1% DMSO (the solvent of the compounds). The other capillary was designated the 'treatment' and filled with 5 μL of 10% sucrose containing 1 mM of CDIAL or a derivative (1% DMSO). The screening concentration (1 mM) was chosen based on preliminary scouting experiments with CDIAL (**1**) that resulted in an antifeedant index of ~0.5. All vials were placed in normal rearing conditions (28°C, 80% relative humidity) for 18–20 h after which the volume of sucrose consumed from each capillary was measured visually with calipers. To determine if a compound possessed significant antifeedant activity, the relative volumes consumed in the treatment vs. control capillaries were compared with paired t-tests ($P < 0.05$). The relative volumes consumed in each capillary were also used to calculate an antifeedant index by subtracting the volume consumed from the treatment capillary from that of the control capillary and dividing by the total volume consumed from both capillaries [21,27,28]. Each derivative was tested on 5–10 vials of 5 adult females. The mean antifeedant indices of the derivatives and CDIAL was compared statistically using a one-way ANOVA (Bonferroni post-test).

Computational modeling

The modeled structure of the AgTRPA1 monomer (amino acid residues: 537–1191) consists of the last 4 repeats of ankyrin repeat (AR) domain, a transmembrane domain, a linker region

between the AR and transmembrane domains, and a C-terminal domain. Several computational approaches were integrated to build different parts of the AgTRPA1 structure, including *ab initio* modeling [29], homology modeling, and loop modeling [30], resulting in a tetrameric structural model of AgTRPA1. This structure was constructed by first forming an AgTRPA1 monomer with GalaxyFill [31] using the cryo-EM structure of hTRPA1 (PDB ID: 3J9P) [32] as a template. Subsequently, a tetramer was assembled with GalaxyHomomer [33] and ZDOCK [34]. Lastly, the tetramer was embedded in a 1-palmitoyl-2-oleoyl-glycero-3-phosphocholine (POPC) bilayer, and the system was minimized/relaxed with short (~10 ns) molecular dynamics (MD) simulations using CHARMM36 force fields [35] and GROMACS [36].

CDIAL was docked to four potential binding pockets near key nucleophilic cysteine and lysine residues (Cys621, Cys641, Cys665 and Lys710 in hTRPA1 and Cys684, Cys704, Lys728 and Lys777 in AgTRPA1) that have been implicated to form covalent bonds with electrophilic agonists [37–39]. Among those, the pocket centered around Cys684 in AgTRPA1 was particularly promising. All docking calculations were performed with the Lamarckian genetic algorithm using Autodock 4.2 [40]. A 96×68×78 grid box with a grid spacing of 0.375 Å centered around each of the four nucleophilic residues defined the region of the protein that the ligands would explore. 500 docking runs were performed for each AgTRPA1 pocket.

Results and discussion

Isolation and identification of bioactive drimane sesquiterpenes

The powdered stem bark of *C. fragrans* (Canellaceae) was extracted with dichloromethane, concentrated, and subjected to silica gel column chromatography and recrystallization to afford cinnamodial (**1**) (Fig 1).

Derivatization of cinnamodial

Cinnamodial (**1**) is one of the approximately more than 80 naturally occurring terpenoids containing an *α,ß*-unsaturated 1,4-dialdehyde functionality [41], specifically **1** belongs to the drimane sesquiterpene class of compounds which includes the structurally similar compounds: warburganal (**2**) and polygodial (**3**) (Fig 1). Unsaturated dialdehyde-containing compounds exhibit diverse bioactivities [42,43], including antimicrobial [44], antifungal [44], molluscicidal [45], and cytotoxicity [46]. Additionally compounds **1**, **2** and **3** are pungent to humans [47–49], possess antifeedant and insecticidal activity [50,51], and agonize Transient Receptor Potential A1 (TRPA1) channels [21,41,49,52,53]. Most biological activities, including the antifeedant activity, of these drimane sesquiterpenes have been attributed to the *α,ß*-unsaturated 1,4-dialdehyde functionality of the molecules, forming adducts with free sulfhydryl groups
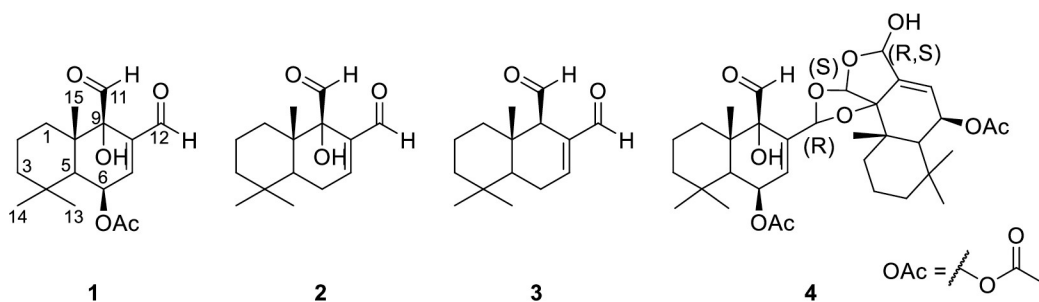

Fig 1. Chemical structures natural drimane-type compounds. Cinnamodial (**1**), warburganal (**2**), polygodial (**3**), capsicodendrin (**4**). Compounds **1**, **3**, and **4** have been isolated from *C. fragrans*.

[54,55] or primary amines such as the ε-amino group of lysine [56]˙ [57]. Our previous results showed that **1** could effectively kill mosquito larvae in an aqueous environment, penetrate the cuticle of adult female mosquitoes, reduce the feeding of mosquitoes when added to a sucrose solution, and reduce the propensity of mosquitoes to blood feed when dried onto the surface of a membrane feeder. Despite these promising results, nonspecific reactions of dialdehydes with endogenous free amines or water may reduce the bioavailability of these compounds. In this work, initial semi-synthetic modification was focused on producing more stable derivatives by replacing the two aldehyde groups while maintaining the *α,ß*-unsaturated system.

Cinnamodial (**1**) was used as starting material for derivatization and analog generation (Fig 2). Pinnick oxidation was employed to generate cinnamodiacid (**5**), wherein the C-11 and C-12 aldehydes were successfully oxidized to the corresponding carboxylic acids. The dimethyl ester derivative **6** was obtained by reacting **5** with (Trimethylsilyl)diazomethane. Reaction of **1** with hydrazine afforded a 2,3-dihydro-3-pyridazinol **7**, which maintained the unsaturated system.

It was envisioned that the more reactive C-12 aldehyde of **1** could be selectively transformed into a methyl ketone by treatment with a methyl Grignard or methyl lithium reagent followed by oxidation of the resulting secondary alcohol. Treatment of **1** with one equivalent of methylmagnesium bromide or methyl lithium instead produced two diastereomeric lactols **8** and **9**, instead of a secondary alcohol. As determined by NMR studies (see experimental), the lactols **8** and **9** differ at the C-12 position depending on whether the C-12 aldehyde of **1** was attacked from the *α* or *ß* face, respectively (Fig 3). Lactol **9** was then converted into the desired compound **10**, with a C-11 aldehyde and C-12 ketone, upon incubation in deuterated chloroform. However, the isomer **8** remained stable in deuterated chloroform and even resisted base-induced lactol-opening / tautomerization with 1,8-Diazabicyclo(5.4.0)undec-7-ene (DBU), see supporting information.
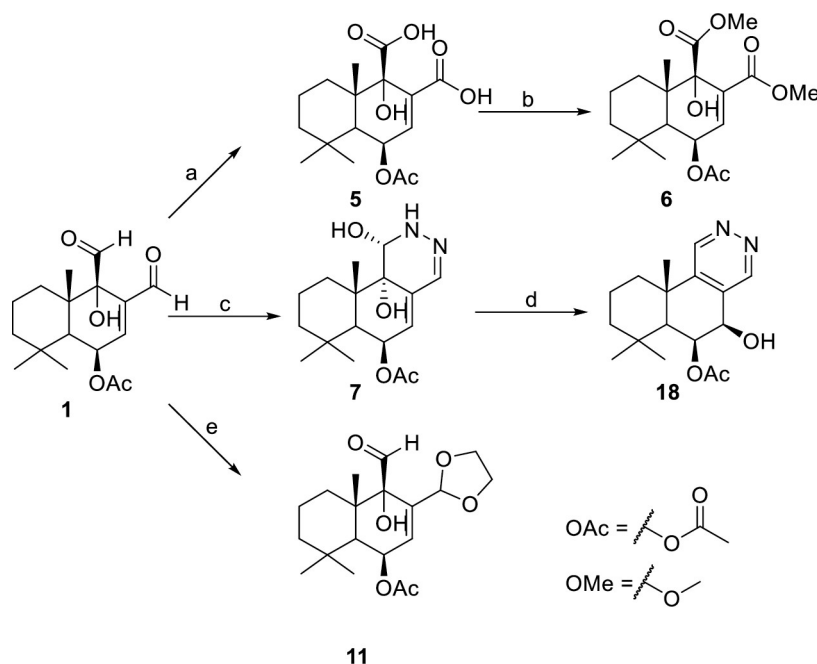

Fig 2. Derivatization of 1 into structural analogues. Reagents and conditions: (a) $NaClO_2$, $NaH_2PO_4 \cdot H_2O$, H_2O_2, MeCN, H_2O, r.t., 24 h; (b) TMS-CHN_2, MeOH:Et_2O, 0 °C, 30 min; (c) H_2N-NH_2, CH_2Cl_2:EtOH, 2 h; (d) MeOH, r.t.; (e) $HOCH_2CH_2OH$, *p*-TsOH, benzene, reflux, 24 h.
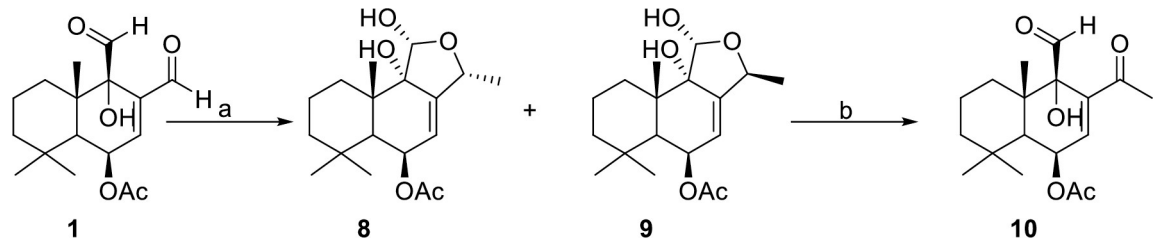
Fig 3. Synthesis of lactols 8 and 9, and formation of 10 from lactol 9. Reagents and conditions: (a) 1 equiv MeMgBr, THF, −78°C, 2 h; (b) CDCl₃, 22 d.

To understand the role of the unsaturated system and confirm the necessity of the C-12 unsaturated aldehyde for its observed biological activity [21], **1** was exposed to one equivalent of ethylene glycol and a catalytic amount of *p*-toluenesulfonic acid in benzene to afford the monoacetal **11** (Fig 2).

Plants and marine organisms have been shown to produce a number of cytotoxic quinones and hydroquinones, including avarone, bolinaquinone, juglone, and lapachol (see S2 Fig in S1 File) [58,59]. Lapachol, isolated from *Tabebuia avellanedae*, and structurally related derivatives have shown modest larvicidal activity against mosquitoes [60,61]. Further modifications of **1** were implemented to prepare a derivative potentially exhibiting mosquito toxicity without antifeedant activity. We had previously shown that the carbon at C-9 bearing a hydroxyl in capsicodendrin (**4**), could be transformed into a ketone by treatment with pyridinium chlorochromate [62]. Therefore, in order to produce a dihydroquinone, **1** was reacted with 5 equivalents of the MeMgBr to alkylate the C-12 aldehyde and to cleave off the C-6 acetyl group providing an isomeric mixture of deacetylated lactols 12α-methyl-pereniporin A and 12ß-methyl-pereniporin A **12** (Fig 4). Pyridinium chlorochromate in dichloromethane was then used to oxidize **12** into a mixture of C-12 isomers of (1'*S/R*)-1'-((8a*S*)-5,5,8a-trimethyl-1,4-dioxo-1,4,4a,5,6,7,8,8a-octahydronaphthalene-2-yl)ethyl formate (**13**).

Model study on the nucleophilic addition of thiol or amino residues to cinnamodial

Studies on natural sesquiterpenes containing the α,ß-unsaturated 1,4-dialdehyde moiety, namely, polygodial (**3**), miogadial (**14**), and isovelleral (**15**) (Fig 5), have suggested that these molecules activate TRPA1 through a mechanism different from that of reactive α,ß-unsaturated aldehydes and isothiocyanates (see S3 Fig in S1 File) [63–67]. Specifically, α,ß-unsaturated aldehydes such as the endogenous ligand (4-hydroxynonenal), the main odiferous
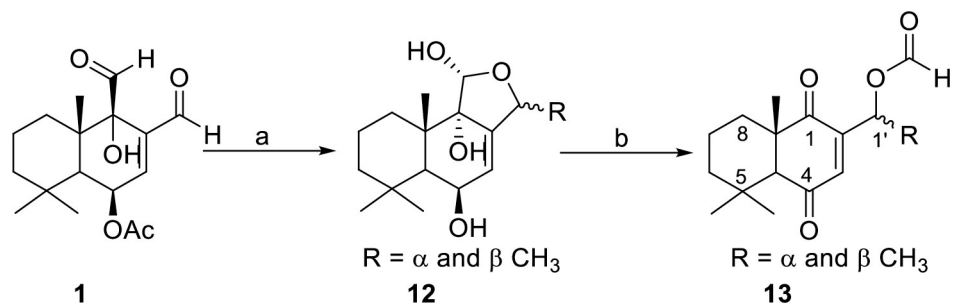

Fig 4. Synthesis of 1,4-dione 13. Reagents and conditions: (a) 5 equiv MeMgBr, THF, −78°C, 2 h; (b) 3.3 equiv PCC, DCM, 0 °C → r.t., 2 h.
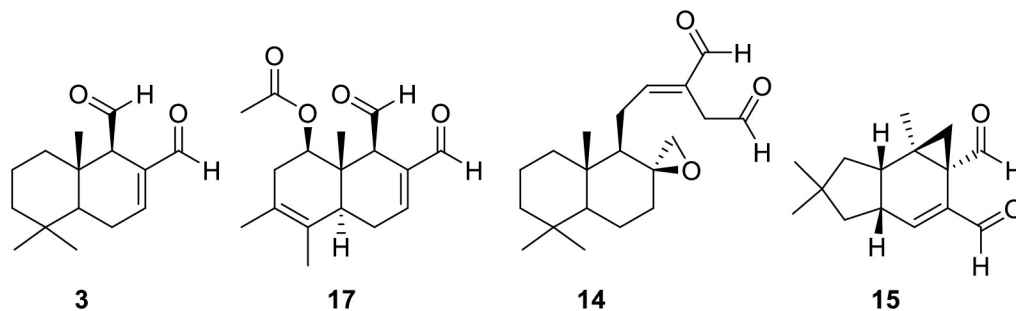
Fig 5. Chemical structures of *α,ß*-unsaturated 1,4-dialdehydes. Polygodial (**3**), 1*ß*-acetoxy-9-deoxy-isomuzigadial (**17**), miogadial (**14**), (+)-isovelleral (**15**).

compound in cinnamon (cinnamaldehyde), and the irritant compound acrolein, activate the TRPA1 channel by covalent modification of N-terminal cysteine residues [37,38,68,69]. Sesquiterpenes with a *α,ß*-unsaturated 1,4-dialdehyde moiety, on the other hand, have been shown to undergo Paal-Knorr condensation reactions with lysine residues [49,53,70].

Since there have been no studies showing the reaction of CDIAL with thiol or amine residues, the reaction of *L*-cysteine methyl ester with CDIAL was used as a model system to study the reaction of **1** with a biological substrate which may in principle react by either thiol or amine addition. CDIAL was treated with *L*-cysteine methyl ester under basic conditions (in pyridine) to afford cinnamothiazolidine (**16**). This adduct likely formed from the initial attack by the primary amine at the more reactive C-12 aldehyde to give the azomethine **A** intermediate, which was then attacked by the thiol to form the thiazolidine **16** (Fig 6). The reaction product and proposed reaction mechanism suggest that the *α,ß*-unsaturated 1,4-dialdehyde **1** may also activate TRPA1 by forming reactive pyrrole-type conjugates with the amino groups present in the protein, as demonstrated for warburganal **2**, polygodial **3**, and 1*ß*-acetoxy-9-deoxy-isomuzigadial (**17**) [49]. Additionally, the attack of the azomethine **A** by the thiol of *L*-cysteine methyl ester suggests that the reactive imine can be attacked by nearby nucleophilic groups, such as the thiol of cysteine and hydroxyl groups of serine or threonine.

Toxicity to larval and adult female mosquitoes

All prepared CDIAL derivatives were screened for 24 h larvicidal activity against 1st instar *Ae. aegypti* (Liverpool, LVP, strain) using a concentration of 100 µM in the rearing water [21]. At this concentration, CDIAL killed *ca*. 70% of the larvae within 24 h (Fig 7A). Nearly all of the CDIAL derivatives showed significantly lower efficacy than CDIAL. However, compounds **10** (86.5%) and **13** (100%) exhibited statistically greater efficacy than CDIAL (Fig 7A).

The derivatives were also screened for 24 h toxicity against adult female *Ae. aegypti* using a dose of 1.5 nmol applied to the thoracic cuticle of each mosquito. At this dose, CDIAL incapacitated 68% of the mosquitoes within 24 h. All of the CDIAL derivatives were significantly less efficacious than CDIAL except for **10**, which was similar to CDIAL in efficacy (74%).

Although the acid **5**, the ester **6**, and the 2,3-dihydro-3-pyridazinol **7** derivatives maintained the *α,ß*-unsaturated functionality of **1**, they were inactive in the toxicity assays against larvae and adult females. The lack of toxicity of **7** can be due to its conversion to the 7-hydroxy-pyridazine **18**, which has been observed in deuterated methanol at room temperature, and also may occur in the carrier solvent used for the bioassays or upon exposure to the rearing water. Since lactol derivatives **8**, **9**, and **12** were not toxic to larvae and adult females, we conclude that the drimane skeleton with C-11 hemiacetal polar head groups is insufficient to elicit mosquito toxicity. These results are consistent with published findings that the biological activity
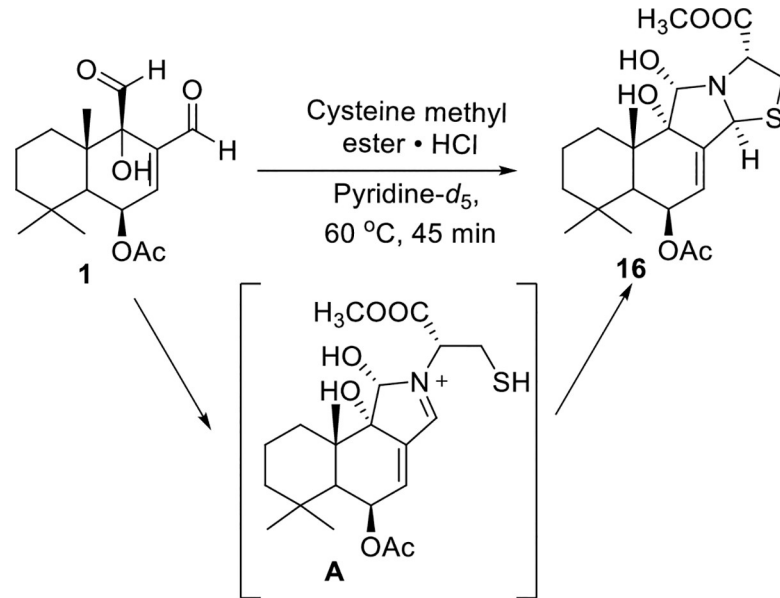
Fig 6. Reaction mechanism. Reaction mechanism of the reaction of **1** with *L*-cysteine methyl ester via a cationic azomethine **A** to form the thiazolidine **16**.

https://doi.org/10.1371/journal.pntd.0008073.g006

of drimane-type compounds are reduced or lost when the aldehyde functionalities are modified [50,71,72]. Acetal protection of the C-12 aldehyde as in compound **11** also abolished the toxicity to larvae and adult females, thus illustrating the crucial role of the conjugated C-12 aldehyde in eliciting a biological response. On the other hand, compound **10**, a C-12 methyl
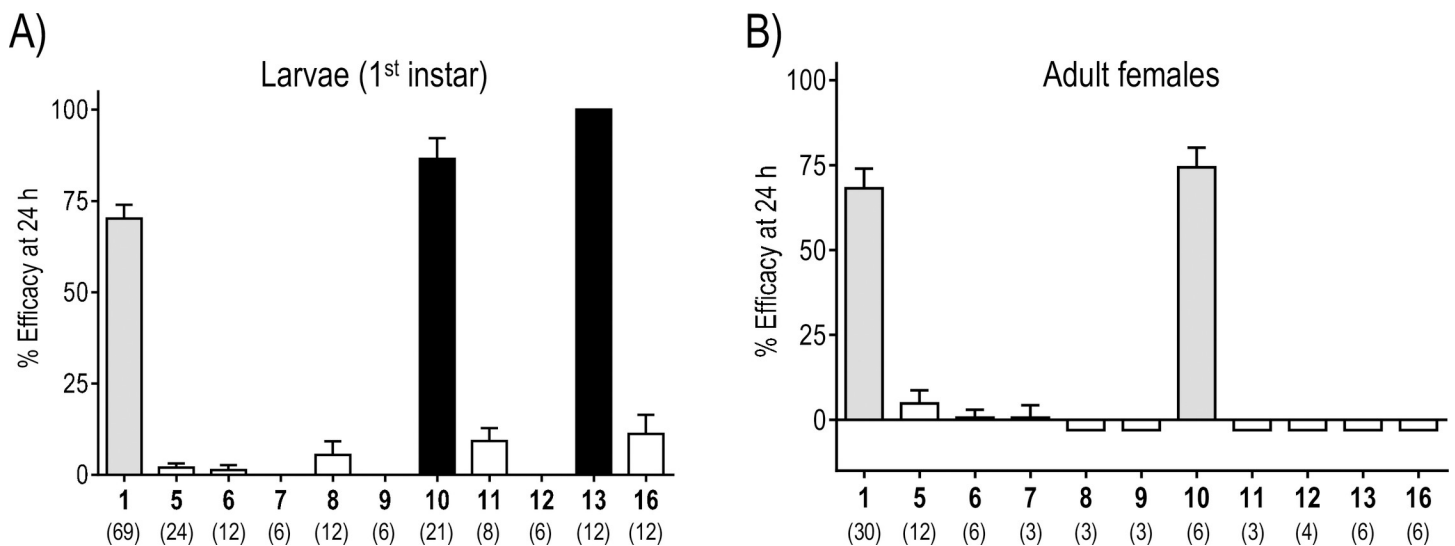

Fig 7. Toxic efficacy of cinnamodial and derivatives against larval (A) and adult female (B) *Ae. aegypti*. The efficacy values were calculated using Abbott's correction to account for control (100% acetone) mortality [26]. In A), compounds were added to the rearing water of 1st instar larvae (100 μM) and efficacy was defined as the percentage of larvae that died within 24 h. In B), compounds were applied to the thoracic cuticle of adult females (1.5 nmol/mosquito) and efficacy was defined as the percentage of adults that were incapacitated (dead or flightless) within 24 h. Values are means ± SEM based on at least 6 replicates of 5 larvae each or 3 replicates of 10 adult females each. The specific numbers of replicates for each are indicated in parentheses below the compound number. Shading indicates statistical categorization of a derivative's efficacy relative to CDIAL as determined by a one-way ANOVA with a Bonferroni post-test: gray = similar (P > 0.05); filled = superior (P < 0.05); open = inferior (P < 0.05).

https://doi.org/10.1371/journal.pntd.0008073.g007

ketone of **1**, exhibited superior and similar efficacy to larvae and adult females, respectively, relative to **1**. Thus, the more stable methyl ketone can effectively replace the aldehyde moiety. Remarkably, the dihydroquinone **13** exhibited superior larvicidal activity to **1** and was 100% effective in the screening experiments (Fig 7A). Additional experiments determined the full concentration-response curves of **1** and **13** to better compare their relative activities (see S4 Fig in S1 File). The EC_{50} of **13** (37.8 µM; 95% C.I. = 34.35–41.5 µM) was ~2.2-times more potent than **1** (82.5 µM; 95% C.I. = 70.7–96.25 µM). Despite the superior larvicidal activity of **13**, it was nominally toxic to adult females. We hypothesized that the chemical modifications resulting in the dihydroquinone preserved the toxicity of the molecule, but may have reduced its ability to penetrate the cuticle of adult females. Thus, we directly injected **13** into the hemolymph of adult females (1.5 nmol/mosquito) to bypass the cuticular barrier. However, even when injected, **13** was weakly toxic to adult females within 24 h (9.8 ± 7.6% efficacy) compared to CDIAL (90.0 ± 5.0% efficacy) ($P < 0.0001$; unpaired t-test; N = 7 replicates of 10 mosquitoes each). Thus, **13** may exploit a larval specific mechanism to induce toxicity or it is more readily detoxified/excreted in adult females vs. larvae. In summary, the relative activities of the analogs observed against larval and adult mosquitoes (Fig 7) indicate the important role of the 1,4-dialdehyde functional group in insecticidal activity.

Antifeedant activity in adult female mosquitoes [26]

A capillary feeding (CAFE) choice bioassay was used to screen the antifeedant activity of the CDIAL derivatives against adult female *Ae. aegypti* (LVP strain) [21,27,28]. Briefly, mosquitoes were presented with two capillaries of 10% sucrose as a food source for 18–20 h; the 'control' capillary was treated with 1% DMSO (the carrier solvent for **1** and its derivatives in this assay) while the 'treatment' capillary was treated with **1** or a derivative thereof at a concentration of 1 mM. With the exception of **8** and **11**, mosquitoes consumed significantly less sucrose from the capillaries treated with the derivatives vs. the control capillaries (paired t-tests; $P < 0.05$), indicative of antifeedant activity. However, the antifeedant efficacy (i.e., antifeedant index) of each derivative was inferior compared to CDIAL (Fig 8).

We have previously shown that the antifeedant activity, but not insecticidal activity, of CDIAL was associated with its modulation of TRPA1 channels [21]. Thus, we suspect that all of the derivatives were inferior agonists of TRPA1 compared to CDIAL. The reduced TRPA1 agonistic activity may be attributable to the reactivity of the unsaturated system of the molecules. Specifically, the unsaturated aldehyde in **1** favors 1,2-addition, while **5**, **6**, and **7** likely favor 1,4-addition. Thus, **1** would be more amenable to direct attack of an amino group on TRPA1 than the other conjugated derivatives. The mosquito antifeedant activities of **5**, **6**, and **7** showed a similar trend to previously reported antifeedant activity of polygodial analogues [42,43]. As mentioned above, the possible conversion of **7** to **18** during the assay may also lead to the reduced activity. The absence of activity in **11** illustrates the necessity of the C-12 conjugated carbonyl group.

Although the derivatives were inferior to CDIAL in the context of antifeedant activity, bioactivity was not completely lost except for **8** and **11** and they still provide some insights into the SAR. For example, among the derivatives, **10** and **12**, were relatively effective antifeedants. The moderate activity of compound **10** may indicate that the C-12 aldehyde can be converted into a methyl ketone without complete loss of antifeedant efficacy. For the lactol **12** it is possible that a ring opening tautomerization affords the C-11 aldehyde and a C-12 conjugated carbonyl.

Unsaturated aldehyde-containing agonists, such as acrolein, are known to react with nucleophilic residues of TRPA1 channels, including cysteine, histidine, and lysine. Several cysteine
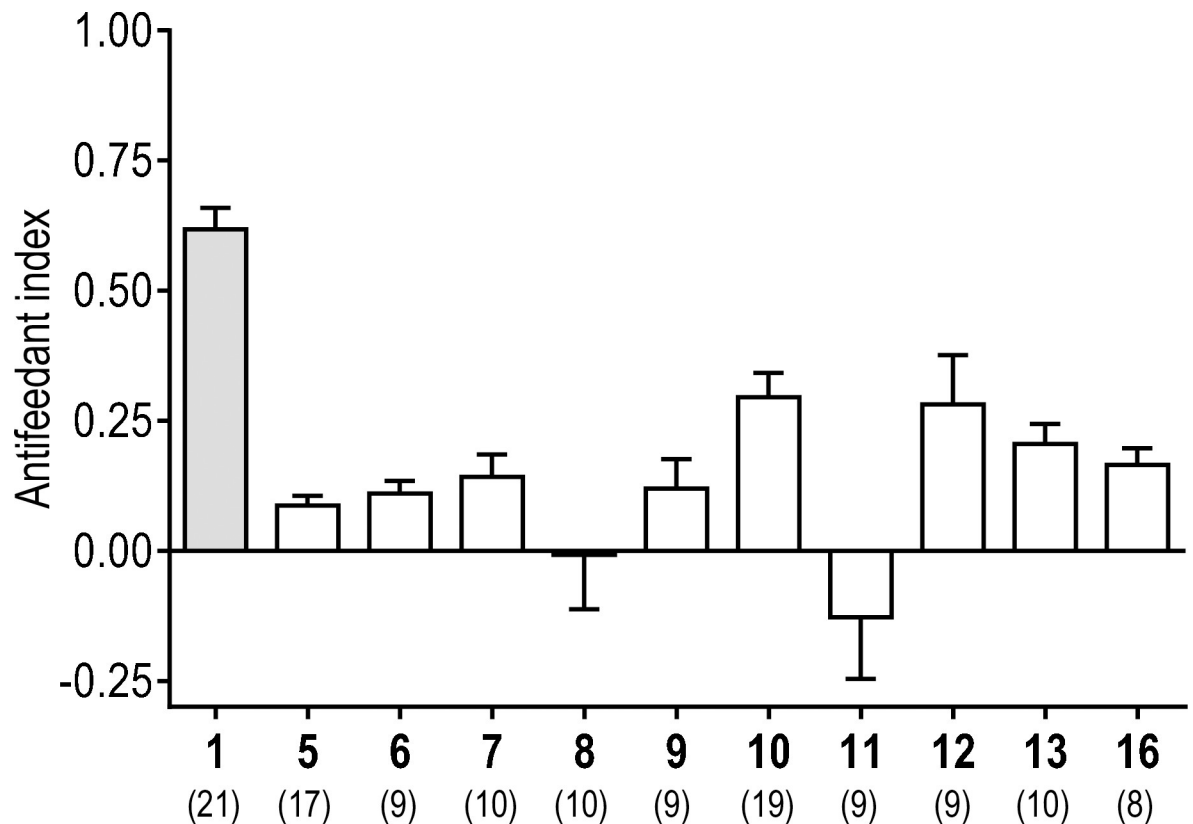
Fig 8. Antifeedant activity of CDIAL and semi-synthetic derivatives as determined via choice CAFE assays in adult female *Ae. aegypti* (LVP strain). Mosquitoes were allowed to feed equally on two capillaries of 10% sucrose with 0.01% trypan blue; the control capillary included 1% DMSO, and the treatment capillary included 1% DMSO and 1mM test compound. The difference in volume consumed between the capillaries was used to calculate the antifeedant activity [21]. Values are means ± SEM based on at least 8 replicates of 5 adult females each. The specific numbers of replicates for each are indicated in parentheses below the compound number. Shading indicates statistical categorization of derivative's efficacy relative to CDIAL as in Fig 7.

https://doi.org/10.1371/journal.pntd.0008073.g008

residues in TRPA1 channels have been identified as potential sites that can form covalent adducts with these agonists [37,38]. However, further mutagenesis experiments also showed that unsaturated dialdehyde-containing sesquiterpenes might not bind to the same sites as those targeted by the small agonists [66]. To shed light on how CDIAL interacts with the mosquito TRPA1 channel and thereby modulating its antifeedant effects, we have developed a structural model of mosquito TRPA1 based on the single-particle cryo-electron microscopy (EM) structure of human TRPA1 (hTRPA1) [32], and then computationally docked CDIAL to the AgTRPA1 structural model. We used the TRPA1 channel of *Anopheles gambiae* (AgTRPA1) as a representative mosquito TRPA1, because it has been previously cloned and shown to be directly activated by CDIAL [21,73]. Moreover, the amino acid identity between AgTRPA1 and the predicted *Ae. aegypti* TRPA1 (AAEL009419) is very high (>83%). In particular, the putative CDIAL binding region we have identified (see below) is over 90% identical between the two species.

Our results suggest that CDIAL binds preferentially to a 'pocket' near Cys684 (Fig 9), a residue in TRPA1 channels that has been implicated to interact with electrophilic agonists [38]. Notably, six lysine residues are located within a radius of 10 Å from Cys684, including Lys656, Lys678, Lys681, Lys728, Lys738 and Lys744. Many of these lysine residues are surrounded by negatively charged residues (Glu or Asp), thereby making them more nucleophilic and likely
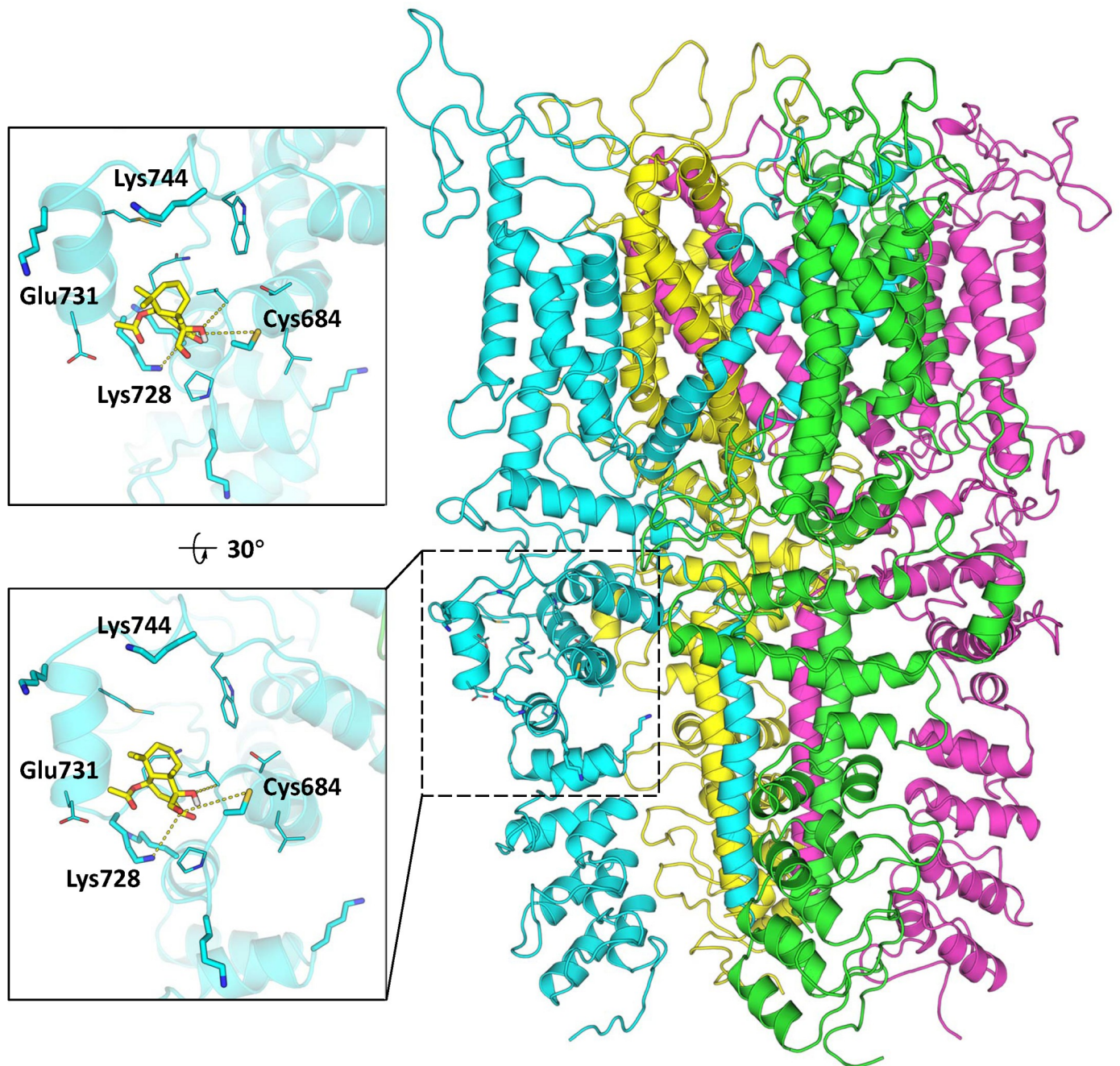
Fig 9. The computationally docked structure of CDIAL (1) in AgTRPA1. The tetrameric AgTRPA1 structure is shown on the right in a cartoon representation. Two zoomed views of the CDIAL binding site are shown on the left. The ligand is shown in a yellow licorice representation and the protein in a cyan cartoon representation. Nearby Cys and Lys residues are labeled.

https://doi.org/10.1371/journal.pntd.0008073.g009

to interact with an electrophile like CDIAL. The dominant predicted CDIAL binding site is located between Cys684 and Lys728 (Fig 9). Analogous to Lys661 in human TRPA1, Lys728 is the closest lysine to Cys684. In these docked poses (Fig 9), the C-12 aldehyde of CDIAL is found close (4.2–5.0 Å) to the amino group of Lys728 that can initiate a nucleophilic attack on C-12 to form an initial CDIAL-AgTRPA1 conjugate, highlighting the importance of the

reactive C-12 aldehyde group. This is consistent with the observation that acetal protection of the C-12 aldehyde in compound 11 abolished its antifeedant activity (Fig 8). Further, given the proximity (~5.0 Å) of the thiol group of Cys684, the polarized C-12 or C-7 of CDIAL may subsequently be attacked by this thiol. Overall, the docking results show a few possible ways in which CDIAL can interact with AgTRPA1, suggesting that the reactions of the *α,ß*-unsaturated 1,4-dialdehyde with nearby amine and thiol side chains (consistent with the formation of thiazolidine when CDIAL was treated with *L*-cysteine methyl ester in pyridine proposed in Fig 6) may be responsible for activating the AgTRPA1 channel. Overall, these preliminary computational results provide a molecular rationale for the importance of the dialdehyde moiety and the *α,ß*-unsaturated carbonyl for CDIAL's antifeedant activity. Nonetheless, due to the high flexibility of the loops shaping the CDIAL binding pocket, our computational studies do not exclude the possibility that other Lys residues such as Lys681 and Lys744 may also be involved in reacting with 1 after some local conformational rearrangements.

Conclusion

The current study has analyzed ten semisynthetic analogs (**5**–**13**, and **16**) of the *α,ß*-unsaturated 1,4-dialdehyde cinnamodial (**1**) to identify the structural contributions of **1** toward its larvicidal, adulticidal and antifeedant activity against *Ae. aegypti*. Two analogs, **10** and **13** exhibited more efficacious toxicity against mosquito larvae than **1**. Moreover, **10** was of similar toxic efficacy against adult females as **1**. These results indicate that the reactive C-12 aldehyde can be substituted with relatively stable moieties, such as an unsaturated methyl ketone **10** or hydroquinone **13**, without sacrificing insecticidal activity. All of the other CDIAL analogs showed that the bicyclic drimane skeleton alone was not sufficient to induce larval or adult toxicity.

Notably, all of the analogs possessed weaker antifeedant activity than **1** regardless of their insecticidal activity. These results support the notion that CDIAL's insecticidal and antifeedant mechanisms of action are independent [21]. While our previous results associated CDIAL's antifeedant activity with its modulation of TRPA1 [21], this work suggests that CDIAL may interact with TRPA1 by an initial nucleophilic attack at C-12 by a lysine residue to form a CDIAL-TRPA1 conjugate. The activated conjugate may then undergo further attack at the C-12 or C-7 of CDIAL by a neighboring thiol or nucleophilic residue [57].

Despite the thorough elucidation of the antifeedant structure-activity relationship against lepidopterans [45,51,56,74,75] and the toxicant activity against insect pests [72,74,76–78] by several groups, this is the first investigation into the observed structure-activity relationship (SAR) of **1** against mosquitoes (Figs 7–9). Overall, we have identified several CDIAL derivatives that confirm the importance of the dialdehyde moiety for mosquitocidal activity and the *α,ß*-unsaturated carbonyl for antifeedant activity. The improved larvicidal activity observed in **10** and **13** suggest that the development of more stable and effective insecticidal CDIAL derivatives is possible. Future studies will focus on developing a comprehensive screening library of CDIAL derivatives and implementation of quantitative SAR to fully elucidate the insecticidal and antifeedant SARs of CDIAL, optimize its bioactivities, and identify its active pharmacophores. The latter may enable the synthesis of relatively simple synthetic molecules with similar or improved insecticidal activity compared to CDIAL, as has been recently accomplished for the spinosyns [79,80].

Supporting information

S1 File. Semi-synthetic cinnamodial analogues supporting information file. Supporting structures, larvicidal concentration-response curve, synthesis, characterization data (including

^{1}H and ^{13}C NMR, IR, and mass spectra), and supporting references.
(DOCX)

Acknowledgments

Author Contributions

Conceptualization: Preston K. Manwill, Megha Kalsi, Xiaolin Cheng, Peter M. Piermarini, Harinantenaina L. Rakotondraibe.

Data curation: Preston K. Manwill, Megha Kalsi, Sijin Wu, Peter M. Piermarini, Harinantenaina L. Rakotondraibe.

Formal analysis: Preston K. Manwill, Megha Kalsi, Sijin Wu, Xiaolin Cheng, Peter M. Piermarini, Harinantenaina L. Rakotondraibe.

Funding acquisition: Peter M. Piermarini, Harinantenaina L. Rakotondraibe.

Investigation: Preston K. Manwill, Megha Kalsi, Erick J. Martinez Rodriguez, Xiaolin Cheng, Peter M. Piermarini, Harinantenaina L. Rakotondraibe.

Methodology: Preston K. Manwill, Megha Kalsi, Erick J. Martinez Rodriguez, Xiaolin Cheng, Peter M. Piermarini, Harinantenaina L. Rakotondraibe.

Project administration: Harinantenaina L. Rakotondraibe.

Resources: Preston K. Manwill, Xiaolin Cheng, Peter M. Piermarini, Harinantenaina L. Rakotondraibe.

Software: Xiaolin Cheng.

Supervision: Xiaolin Cheng, Peter M. Piermarini, Harinantenaina L. Rakotondraibe.

Validation: Xiaolin Cheng, Peter M. Piermarini, Harinantenaina L. Rakotondraibe.

Visualization: Preston K. Manwill, Megha Kalsi, Sijin Wu, Xiaolin Cheng, Peter M. Piermarini, Harinantenaina L. Rakotondraibe.

Writing – original draft: Preston K. Manwill.

Writing – review & editing: Preston K. Manwill, Xiaolin Cheng, Peter M. Piermarini, Harinantenaina L. Rakotondraibe.

References

1. WHO | Global vector control response 2017–2030. Geneva: World Health Organization; 2017. Available: http://www.who.int/vector-control/publications/global-control-response/en/

2. WHO | Mosquito-borne diseases. In: WHO [Internet]. [cited 30 Dec 2017]. Available: http://www.who.int/neglected_diseases/vector_ecology/mosquito-borne-diseases/en/

3. Bhatt S, Gething PW, Brady OJ, Messina JP, Farlow AW, Moyes CL, et al. The global distribution and burden of dengue. Nature. 2013; 496: 504–507. https://doi.org/10.1038/nature12060 PMID: 23563266

4. Weaver SC, Lecuit M. Chikungunya Virus and the Global Spread of a Mosquito-Borne Disease. N Engl J Med. 2015; 372: 1231–1239. https://doi.org/10.1056/NEJMra1406035 PMID: 25806915

5. Fauci AS, Morens DM. Zika Virus in the Americas—Yet Another Arbovirus Threat. N Engl J Med. 2016; 374: 601–604. https://doi.org/10.1056/NEJMp1600297 PMID: 26761185

6. Guy B, Briand O, Lang J, Saville M, Jackson N. Development of the Sanofi Pasteur tetravalent dengue vaccine: One more step forward. Vaccine. 2015; 33: 7100–7111. https://doi.org/10.1016/j.vaccine.2015.09.108 PMID: 26475445

7. Vannice KS, Durbin A, Hombach J. Status of vaccine research and development of vaccines for dengue. Vaccine. 2016; 34: 2934–2938. https://doi.org/10.1016/j.vaccine.2015.12.073 PMID: 26973072

8. Huang Y-JS, Higgs S, Vanlandingham DL. Biological Control Strategies for Mosquito Vectors of Arboviruses. Insects. 2017; 8: 21. https://doi.org/10.3390/insects8010021 PMID: 28208639

9. Matthews G. Integrated Vector Management: Controlling Vectors of Malaria and Other Insect Vector Borne Diseases. 1 ed. Chichester, West Sussex, UK: Wiley-Blackwell; 2011.

10. Beyenbach KW, Yu Y, Piermarini PM, Denton J. Targeting renal epithelial channels for the control of insect vectors. Tissue Barriers. 2015; 3: e1081861. https://doi.org/10.1080/21688370.2015.1081861 PMID: 26716074

11. Vijverberg HPM, van den Bercken J. Neurotoxicological Effects and the Mode of Action of Pyrethroid Insecticides. Crit Rev Toxicol. 1990; 21: 105–126. https://doi.org/10.3109/10408449009089875 PMID: 1964560

12. Fukuto TR. Mechanism of action of organophosphorus and carbamate insecticides. Environ Health Perspect. 1990; 87: 245–254. https://doi.org/10.1289/ehp.9087245 PMID: 2176588

13. Simon-Delso N, Amaral-Rogers V, Belzunces LP, Bonmatin JM, Chagnon M, Downs C, et al. Systemic insecticides (neonicotinoids and fipronil): trends, uses, mode of action and metabolites. Environ Sci Pollut Res. 2015; 22: 5–34. https://doi.org/10.1007/s11356-014-3470-y PMID: 25233913

14. Karabelas AJ, Plakas KV, Solomou ES, Drossou V, Sarigiannis DA. Impact of European legislation on marketed pesticides—A view from the standpoint of health impact assessment studies. Environ Int. 2009; 35: 1096–1107. https://doi.org/10.1016/j.envint.2009.06.011 PMID: 19632722

15. Dayan FE, Cantrell CL, Duke SO. Natural products in crop protection. Bioorg Med Chem. 2009; 17: 4022–4034. https://doi.org/10.1016/j.bmc.2009.01.046 PMID: 19216080

16. Hemingway J, Hawkes NJ, McCarroll L, Ranson H. The molecular basis of insecticide resistance in mosquitoes. Insect Biochem Mol Biol. 2004; 34: 653–665. https://doi.org/10.1016/j.ibmb.2004.03.018 PMID: 15242706

17. Maharaj R. Global trends in insecticide resistance and impact on disease vector control measures. Open Access Insect Physiol. 2011; 3: 27–33. https://doi.org/10.2147/OAIP.S8620

18. Hemingway J, Beaty BJ, Rowland M, Scott TW, Sharp BL. The Innovative Vector Control Consortium: improved control of mosquito-borne diseases. Trends Parasitol. 22: 308–312. https://doi.org/10.1016/j.pt.2006.05.003 PMID: 16713358

19. Zaim M, Aitio A, Nakashima N. Safety of pyrethroid-treated mosquito nets. Med Vet Entomol. 2000; 14: 1–5. https://doi.org/10.1046/j.1365-2915.2000.00211.x PMID: 10759305

20. Casida JE. Pyrethrum flowers and pyrethroid insecticides. Environ Health Perspect. 1980; 34: 189–202. https://doi.org/10.1289/ehp.8034189 PMID: 6993201

21. Inocente EA, Shaya M, Acosta N, Rakotondraibe LH, Piermarini PM. A natural agonist of mosquito TRPA1 from the medicinal plant Cinnamosma fragrans that is toxic, antifeedant, and repellent to the yellow fever mosquito Aedes aegypti. PLoS Negl Trop Dis. 2018; 12: e0006265. https://doi.org/10.1371/journal.pntd.0006265 PMID: 29425195

22. Piermarini PM, Hine RM, Schepel M, Miyauchi J, Beyenbach KW. Role of an apical K,Cl cotransporter in urine formation by renal tubules of the yellow fever mosquito (Aedes aegypti). Am J Physiol—Regul Integr Comp Physiol. 2011; 301: R1318–R1337. https://doi.org/10.1152/ajpregu.00223.2011 PMID: 21813871

23. Pridgeon JW, Becnel JJ, Clark GG, Linthicum KJ. A High-Throughput Screening Method to Identify Potential Pesticides for Mosquito Control. J Med Entomol. 2009; 46: 335–341. https://doi.org/10.1603/033.046.0219 PMID: 19351085

24. Swale DR, Engers DW, Bollinger SR, Gross A, Inocente EA, Days E, et al. An insecticide resistance-breaking mosquitocide targeting inward rectifier potassium channels in vectors of Zika virus and malaria. 2016; 6: 36954.

25. Raphemot R, Rouhier MF, Hopkins CR, Gogliotti RD, Lovell KM, Hine RM, et al. Eliciting Renal Failure in Mosquitoes with a Small-Molecule Inhibitor of Inward-Rectifying Potassium Channels. PLOS ONE. 2013; 8: e64905. https://doi.org/10.1371/journal.pone.0064905 PMID: 23734226

26. Abbott WS. A Method of Computing the Effectiveness of an Insecticide. J Econ Entomol. 1925; 18: 265–267. https://doi.org/10.1093/jee/18.2.265a

27. Corfas RA, Vosshall LB. The cation channel TRPA1 tunes mosquito thermotaxis to host temperatures. eLife. 2015; 4: e11750. https://doi.org/10.7554/eLife.11750 PMID: 26670734

28. Ja WW, Carvalho GB, Mak EM, de la Rosa NN, Fang AY, Liong JC, et al. Prandiology of *Drosophila* and the CAFE assay. Proc Natl Acad Sci. 2007; 104: 8253–8256. https://doi.org/10.1073/pnas.0702726104 PMID: 17494737

29. Das R, Baker D. Macromolecular Modeling with Rosetta. Annu Rev Biochem. 2008; 77: 363–382. https://doi.org/10.1146/annurev.biochem.77.062906.171838 PMID: 18410248

30. Fiser A, Do RKG, Šali A. Modeling of loops in protein structures. Protein Sci. 2000; 9: 1753–1773. https://doi.org/10.1110/ps.9.9.1753 PMID: 11045621

31. Coutsias EA, Seok C, Jacobson MP, Dill KA. A kinematic view of loop closure. J Comput Chem. 2004; 25: 510–528. https://doi.org/10.1002/jcc.10416 PMID: 14735570

32. Paulsen CE, Armache J-P, Gao Y, Cheng Y, Julius D. Structure of the TRPA1 ion channel suggests regulatory mechanisms. Nature. 2015; 520: 511–517. https://doi.org/10.1038/nature14367 PMID: 25855297

33. Baek M, Park T, Heo L, Park C, Seok C. GalaxyHomomer: a web server for protein homo-oligomer structure prediction from a monomer sequence or structure. Nucleic Acids Res. 2017; 45: W320–W324. https://doi.org/10.1093/nar/gkx246 PMID: 28387820

34. Pierce BG, Wiehe K, Hwang H, Kim B-H, Vreven T, Weng Z. ZDOCK server: interactive docking prediction of protein–protein complexes and symmetric multimers. Bioinformatics. 2014; 30: 1771–1773. https://doi.org/10.1093/bioinformatics/btu097 PMID: 24532726

35. MacKerell AD, Bashford D, Bellott M, Dunbrack RL, Evanseck JD, Field MJ, et al. All-atom empirical potential for molecular modeling and dynamics studies of proteins. J Phys Chem B. 1998; 102: 3586–3616. https://doi.org/10.1021/jp973084f PMID: 24889800

36. Hess B, Kutzner C, van der Spoel D, Lindahl E. GROMACS 4: Algorithms for Highly Efficient, Load-Balanced, and Scalable Molecular Simulation. J Chem Theory Comput. 2008; 4: 435–447. https://doi.org/10.1021/ct700301q PMID: 26620784

37. Hinman A, Chuang H, Bautista DM, Julius D. TRP channel activation by reversible covalent modification. Proc Natl Acad Sci. 2006; 103: 19564–19568. https://doi.org/10.1073/pnas.0609598103 PMID: 17164327

38. Macpherson LJ, Dubin AE, Evans MJ, Marr F, Schultz PG, Cravatt BF, et al. Noxious compounds activate TRPA1 ion channels through covalent modification of cysteines. Nature. 2007; 445: 541–545. https://doi.org/10.1038/nature05544 PMID: 17237762

39. Bahia PK, Parks TA, Stanford KR, Mitchell DA, Varma S, Stevens SM, et al. The exceptionally high reactivity of Cys 621 is critical for electrophilic activation of the sensory nerve ion channel TRPA1. J Gen Physiol. 2016; 147: 451–465. https://doi.org/10.1085/jgp.201611581 PMID: 27241698

40. Goodsell DS, Morris GM, Olson AJ. Automated docking of flexible ligands: Applications of autodock. J Mol Recognit. 1996; 9: 1–5. https://doi.org/10.1002/(sici)1099-1352(199601)9:1<1::aid-jmr241>3.0.co;2-6 PMID: 8723313

41. Sterner O, Szallasi A. Novel natural vanilloid receptor agonists: new therapeutic targets for drug development. Trends Pharmacol Sci. 1999; 20: 459–465. https://doi.org/10.1016/s0165-6147(99)01393-0 PMID: 10542446

42. Jansen BJM, de Groot A. The occurrence and biological activity of drimane sesquiterpenoids. Nat Prod Rep. 1991; 8: 309–318. https://doi.org/10.1039/np9910800309 PMID: 1945065

43. Jansen BJM, de Groot Ae. Occurrence, biological activity and synthesis of drimane sesquiterpenoids. Nat Prod Rep. 2004; 21: 449–477. https://doi.org/10.1039/b311170a PMID: 15282630

44. Taniguchi M, Adachi T, Oi S, Kimura A, Katsumura S, Isoe S, et al. Structure-Activity Relationship of the *Warburgia* Sesquiterpene Dialdehydes. Agric Biol Chem. 1984; 48: 73–78. https://doi.org/10.1271/bbb1961.48.73

45. Nakanishi K, Kubo I. Studies on Warburganal, Muzigadial and Related Compounds. Isr J Chem. 1977; 16: 28–31. https://doi.org/10.1002/ijch.197700009

46. Montenegro I, Tomasoni G, Bosio C, Quiñones N, Madrid A, Carrasco H, et al. Study on the Cytotoxic Activity of Drimane Sesquiterpenes and Nordrimane Compounds against Cancer Cell Lines. Molecules. 2014; 19: 18993–19006. https://doi.org/10.3390/molecules191118993 PMID: 25412045

47. Govindarajan VS. Pungency: The Stimuli and Their Evaluation. Food Taste Chemistry. AMERICAN CHEMICAL SOCIETY; 1979. pp. 53–92. https://doi.org/10.1021/bk-1979-0115.ch003

48. Kubo I, Ganjian I. Insect antifeedant terpenes, hot-tasting to humans. Experientia. 1981; 37: 1063–1064. https://doi.org/10.1007/bf02085009 PMID: 7308389

49. Mathie K, Lainer J, Spreng S, Dawid C, Andersson DA, Bevan S, et al. Structure–Pungency Relationships and TRP Channel Activation of Drimane Sesquiterpenes in Tasmanian Pepper (Tasmannia lanceolata). J Agric Food Chem. 2017; 65: 5700–5712. https://doi.org/10.1021/acs.jafc.7b02356 PMID: 28657737

50. Blaney WM, Simmonds MSJ, Ley SV, Katz RB. An electrophysiological and behavioural study of insect antifeedant properties of natural and synthetic drimane-related compounds. Physiol Entomol. 1987; 12: 281–291. https://doi.org/10.1111/j.1365-3032.1987.tb00752.x

51. Kubo I, Miura I, Pettei MJ, Lee Y-W, Pilkiewicz F, Nakanishi K. Muzigadial and warburganal, potent anti-fungal antiyeast, and African army worm antifeedant agents. Tetrahedron Lett. 1977; 18: 4553–4556. https://doi.org/10.1016/S0040-4039(01)83566-8

52. Andre E, Ferreira J, Malheiros Â, Yunes RA, Calixto JB. Evidence for the involvement of vanilloid receptor in the antinociception produced by the dialdeydes unsaturated sesquiterpenes polygodial and drimanial in rats. Neuropharmacology. 2004; 46: 590–597. https://doi.org/10.1016/j.neuropharm.2003.10.008 PMID: 14975683

53. Dasari R, De Carvalho A, Medellin DC, Middleton KN, Hague F, Volmar MNM, et al. Synthetic and Biological Studies of Sesquiterpene Polygodial: Activity of 9-Epipolygodial against Drug-Resistant Cancer Cells. ChemMedChem. 2015; 10: 2014–2026. https://doi.org/10.1002/cmdc.201500360 PMID: 26434977

54. Ma W-C. Alterations of chemoreceptor function in army worm larvae (Spodoptera exempta) by a plant-derived sesquiterpenoid and by sulfhydryl reagents. Physiol Entomol. 1977; 2: 199–207. https://doi.org/10.1111/j.1365-3032.1977.tb00104.x

55. Singer G, Rozental JM, Norris DM. Sulphydryl groups and the quinone receptor in insect olfaction and gustation. Nature. 1975; 256: 222. https://doi.org/10.1038/256222a0 PMID: 1152992

56. D'Ischia M, Prota G, Sodano G. Reaction of polygodial with primary amines: an alternative explanation to the antifeedant activity. Tetrahedron Lett. 1982; 23: 3295–3298. https://doi.org/10.1016/S0040-4039(00)87596-6

57. Fritz GL, Mills GD, Warthen JD, Waters RM. Reimer-Tiemann adducts as potential insect antifeedant agents Reviewing the structure-activity relationship theory of the antifeedant, warburganal. J Chem Ecol. 1989; 15: 2607–2623. https://doi.org/10.1007/BF01014720 PMID: 24271675

58. Gordaliza M. Cytotoxic Terpene Quinones from Marine Sponges. Mar Drugs Mar Drugs. 2010; 8, 8: 2849, 2849–2870. https://doi.org/10.3390/md8122849 PMID: 21339953

59. Ribeiro KAL, de Carvalho CM, Molina MT, Lima EP, López-Montero E, Reys JRM, et al. Activities of naphthoquinones against Aedes aegypti (Linnaeus, 1762) (Diptera: Culicidae), vector of dengue and Biomphalaria glabrata (Say, 1818), intermediate host of *Schistosoma mansoni*. Acta Trop. 2009; 111: 44–50. https://doi.org/10.1016/j.actatropica.2009.02.008 PMID: 19426662

60. Kim M-G, Jeon J-H, Lee H-S. Larvicidal Activity of the Active Constituent Isolated from *Tabebuia avella-nedae* Bark and Structurally Related Derivatives against Three Mosquito Species. J Agric Food Chem. 2013; 61: 10741–10745. https://doi.org/10.1021/jf403679h PMID: 24144401

61. De Sousa DP, Vieira YW, Uliana MP, Melo MA, Brocksom TJ, Cavalcanti SCH. Larvicidal activity of para-Benzoquinones. Parasitol Res. 2010; 107: 741–745. https://doi.org/10.1007/s00436-010-1942-7 PMID: 20549237

62. He D, Slebodnick C, Rakotondraibe LH. Bioactive drimane sesquiterpenoids and aromatic glycosides from *Cinnamosma fragrans*. Bioorg Med Chem Lett. 2017; 27: 1754–1759. https://doi.org/10.1016/j.bmcl.2017.02.067 PMID: 28274626

63. Szallasi A, Bíró T, Modarres S, Garlaschelli L, Petersen M, Klusch A, et al. Dialdehyde sesquiterpenes and other terpenoids as vanilloids. Eur J Pharmacol. 1998; 356: 81–89. https://doi.org/10.1016/s0014-2999(98)00514-7 PMID: 9761427

64. Fujita K, Kubo I. Multifunctional action of antifungal polygodial against *Saccharomyces cerevisiae*: Involvement of pyrrole formation on cell surface in antifungal action. Bioorg Med Chem. 2005; 13: 6742–6747. https://doi.org/10.1016/j.bmc.2005.07.023 PMID: 16122929

65. Moreno-Osorio L, Cortés M, Armstrong V, Bailén M, González-Coloma A. Antifeedant activity of some polygodial derivatives. Z Naturforschung C J Biosci. 2008; 63: 215–220.

66. Escalera J, Hehn CA von, Bessac BF, Sivula M, Jordt S-E. TRPA1 Mediates the Noxious Effects of Natural Sesquiterpene Deterrents. J Biol Chem. 2008; 283: 24136–24144. https://doi.org/10.1074/jbc.M710280200 PMID: 18550530

67. Iwasaki Y, Tanabe M, Kayama Y, Abe M, Kashio M, Koizumi K, et al. Miogadial and miogatrial with α,β-unsaturated 1,4-dialdehyde moieties—Novel and potent TRPA1 agonists. Life Sci. 2009; 85: 60–69. https://doi.org/10.1016/j.lfs.2009.04.017 PMID: 19409911

68. Takahashi N, Mizuno Y, Kozai D, Yamamoto S, Kiyonaka S, Shibata T, et al. Molecular characterization of TRPA1 channel activation by cysteine-reactive inflammatory mediators. Channels. 2008; 2: 287–298. https://doi.org/10.4161/chan.2.4.6745 PMID: 18769139

69. Salazar H, Llorente I, Jara-Oseguera A, García-Villegas R, Munari M, Gordon SE, et al. A single N-terminal cysteine in TRPV1 determines activation by pungent compounds from onion and garlic. Nat Neurosci. 2008; 11: 255–261. https://doi.org/10.1038/nn2056 PMID: 18297068

70. Kornienko A, Clair JJL. Covalent modification of biological targets with natural products through Paal–Knorr pyrrole formation. Nat Prod Rep. 2017; 34: 1051–1060. https://doi.org/10.1039/c7np00024c PMID: 28808718

71. Derita M, Montenegro I, Garibotto F, Enriz RD, Fritis MC, Zacchino SA. Structural Requirements for the Antifungal Activities of Natural Drimane Sesquiterpenes and Analogues, Supported by Conformational and Electronic Studies. Molecules. 2013; 18: 2029–2051. https://doi.org/10.3390/molecules18022029 PMID: 23385340

72. Montenegro I, Pino L, Werner E, Madrid A, Espinoza L, Moreno L, et al. Comparative Study on the Larvicidal Activity of Drimane Sesquiterpenes and Nordrimane Compounds against Drosophila melanogaster til-til. Molecules. 2013; 18: 4192–4208. https://doi.org/10.3390/molecules18044192 PMID: 23612472

73. Wang G, Qiu YT, Lu T, Kwon H-W, Jason Pitts R, Van Loon JJA, et al. *Anopheles gambiae* TRPA1 is a heat-activated channel expressed in thermosensitive sensilla of female antennae. Eur J Neurosci. 2009; 30: 967–974. https://doi.org/10.1111/j.1460-9568.2009.06901.x PMID: 19735290

74. Kubo I, Lee Y-W, Pettei M, Pilkiewicz F, Nakanishi K. Potent army worm antifeedants from the east African *Warburgia* plants. J Chem Soc Chem Commun. 1976; 0: 1013–1014. https://doi.org/10.1039/C39760001013

75. Meinwald J, Prestwich GD, Nakanishi K, Kubo I. Chemical Ecology: Studies from East Africa. Science. 1978; 199: 1167–1173. https://doi.org/10.1126/science.199.4334.1167 PMID: 17745589

76. Asakawa Y, Dawson GW, Griffiths DC, Lallemand J-Y, Ley SV, Mori K, et al. Activity of drimane antifeedants and related compounds against aphids, and comparative biological effects and chemical reactivity of (−)- and (+)-polygodial. J Chem Ecol. 1988; 14: 1845–1855. https://doi.org/10.1007/BF01013481 PMID: 24277098

77. Zapata N, Vargas M, Medina P, Viñuela E, Rodríguez B, Fereres A. The activity of a selected extract of *Drimys winteri* bark and polygodial on settling and probing behavior of the lettuce aphid *Nasonovia ribisnigri*. Phytoparasitica. 2010; 38: 191–199. https://doi.org/10.1007/s12600-010-0087-7

78. Gols GJZ, van Loon JJA, Messchendorp L. Antifeedant and toxic effects of drimanes on Colorado potato beetle larvae. Entomol Exp Appl. 1996; 79: 69–76. https://doi.org/10.1111/j.1570-7458.1996.tb00810.x

79. Crouse GD, Demeter DA, Samaritoni G, McLeod CL, Sparks TC. De Novo Design of Potent, Insecticidal Synthetic Mimics of the Spinosyn Macrolide Natural Products. Sci Rep. 2018; 8: 1–6. https://doi.org/10.1038/s41598-017-17765-5

80. Sparks TC, Crouse GD, Demeter DA, Samaritoni G, McLeod CL. Discovery of highly insecticidal synthetic spinosyn mimics–CAMD enabled *de novo* design simplifying a complex natural product. Pest Manag Sci. 2019; 75: 309–313. https://doi.org/10.1002/ps.5217 PMID: 30242953